

Contribution of alpha cluster exchange to elastic and inelastic $^{16}\text{O} + ^{20}\text{Ne}$ scattering*

R. Stock

Fachbereich Physik, Universität Marburg, Marburg, West Germany

U. Jahnke,[†] D. L. Hendrie, J. Mahoney, C. F. Maguire,[‡] W. F. W. Schneider,[§]

D. K. Scott, and G. Wolschin[¶]

Lawrence Berkeley Laboratory, Berkeley, California 94720

(Received 25 June 1976)

Angular distributions for elastic and inelastic transitions in $^{20}\text{Ne} + ^{16}\text{O}$ scattering have been measured at $E(^{20}\text{Ne}) = 50$ MeV. For the 0^+ , 2^+ , and 4^+ members of the ^{20}Ne ground-state rotational band, the angular distributions exhibit pronounced backward peaking characteristic of an α -cluster exchange mechanism. The analysis of the ground-state transition in the first-order elastic transfer model yields no satisfactory fit although microscopic cluster form factors and full recoil corrections are employed. A coupled channels calculation for the 0^+ , 2^+ , and 4^+ transitions reveals very strong coupling effects, indicating that the coherent superposition of first-order optical model and distorted-wave Born-approximation amplitudes may not be an adequate model for these reactions.

[NUCLEAR REACTIONS $^{16}\text{O}(^{20}\text{Ne}, ^{16}\text{O})$ and $^{16}\text{O}(^{20}\text{Ne}, ^{20}\text{Ne})$, elastic and inelastic transfer; $E = 50$ MeV; measured $\sigma(E_f, \theta)$; optical model + DWBA, and CCBA analyses.]

I. INTRODUCTION

Several recent studies of the ^{20}Ne ground state rotational band in microscopic α -cluster plus core models have led to the conclusion that it may be characterized as an α -particle-like configuration of s - d shell nucleons rotating around a spherical ^{16}O core.¹⁻⁶ Furthermore, these calculations showed that the core may be, to a good approximation, identified with the ground state of ^{16}O . In the scattering of ^{20}Ne from ^{16}O , the exchange of the α cluster between two identical ^{16}O cores should then contribute to the observed cross sections.⁷ Viewed as a simple one-step direct reaction mechanism, the cluster can remain with the ^{16}O core of the incident ^{20}Ne projectile leading to elastic or inelastic scattering; in the latter case, the angular momentum transfer l of the reaction arises from the excitation of cluster rotation with angular momentum $L = l$ leading to a final ^{20}Ne state with $J = L$. This part of the reaction may be described by optical model and distorted-wave Born-approximation (DWBA) amplitudes, respectively. In a coupled channels treatment, the corresponding amplitudes include the effect of virtual transitions between the rotational states of ^{20}Ne in the reaction. If, on the other hand, the cluster is exchanged to the ^{16}O target nucleus forming one of the ^{20}Ne rotational states, the final reaction products are the same, but the different kinematical situations in the two reaction paths make their contributions to the cross section show up in different regions of scattering angles.

At reaction energies above the Coulomb barrier the nonexchange cross section is forward peaked, whereas the exchange process contributes predominantly at backward angles.^{7,8} The amplitude of the exchange path may be obtained in the DWBA approximation as an α transfer process $^{16}\text{O}(^{20}\text{Ne}, ^{16}\text{O})^{20}\text{Ne}$, where the transferred angular momentum equals the spin of the ^{20}Ne final state.

In a fully antisymmetric treatment of the reaction both contributions would be automatically included along with other, more complicated mechanisms. As a first approximation for the transition to the ground states of both ^{20}Ne and ^{16}O , a coherent superposition of the elastic scattering amplitude obtained from the optical model with a DWBA, $l = 0$ α -transfer amplitude appeared worthwhile. Such a treatment has been successfully applied^{9,10} to the scattering of ^{11}B from ^{12}C , and ^{28}Si from ^{29}Si , where a single nucleon is exchanged between identical cores. The contribution of "elastic transfer" was demonstrated to lead to a substantial backward rise in the cross sections and to a characteristic interference structure in the region around 90° scattering angle where both amplitudes overlap. In addition to explaining the observed backward rise in the angular distributions, this analysis offered a new way of determining the spectroscopic factor of the transferred nucleon or cluster in the nuclear states involved. In conventional transfer reactions the *cross section* is proportional to the spectroscopic factor S of the transferred object in the final (stripping) or initial (pickup) nuclear state. In elastic trans-

fer, the *amplitude* is proportional to S because the transferred nucleons are stripped from the initial and picked up by the final nuclear states which are identical. In the case of the $^{20}\text{Ne} + ^{16}\text{O}$ ground-state transition, the exchange amplitude is proportional to the square of the α relative motion form factor¹

$$\chi(R) = \binom{20}{4}^{-1/2} \int \Phi^*(^{16}\text{O}) \Phi^*(\alpha) \Phi(^{20}\text{Ne}) d\xi, \quad (1)$$

where R is the relative distance between ^{16}O and α , and the Φ are antisymmetric internal wave functions. The α spectroscopic factor of ^{20}Ne is given by

$$S_\alpha^{\text{c.m.}} = \int |\chi(R)|^2 R^2 dR, \quad (2)$$

therefore the cross section at the very backward angles, where interference with the nonexchange contribution may be neglected, is proportional to S_α^2 . Furthermore, the interference structure at intermediate angles is very sensitive to S_α . This quantity can thus be determined from measured absolute cross sections more sensitively than in a transfer reaction like $^{16}\text{O}(^6\text{Li}, d)^{20}\text{Ne}$.

In order to test the prediction of microscopic models that the members of the ^{20}Ne ground state rotational band are α cluster configurations with more or less constant α -particle spectroscopic factors, we have measured angular distributions of the reactions $^{20}\text{Ne} + ^{16}\text{O} \rightarrow ^{16}\text{O}(\text{g.s.}) + ^{20}\text{Ne}(\text{O}^+\text{g.s.}, 2^+, 4^+)$ at an incident ^{20}Ne energy of 50 MeV which is slightly above the Coulomb barrier. The analysis of the ground-state transition was performed with various microscopic ^{20}Ne cluster wave functions^{4,5} and a superposition of optical model (OM) and DWBA transfer amplitudes; recoil effects were included in the DWBA formalism.¹¹ As we shall show in the following sections, this analysis can qualitatively reproduce the ground-state transition data, lending support to the hypothesis of an α -elastic transfer mechanism. However, the limitations and ambiguities inherent in the first order OM+DWBA approximation render impossible an accurate determination of the α spectroscopic factor, calling for a more consistent treatment of the reaction mechanism.

It did not appear worthwhile, therefore, to analyze the 2^+ and 4^+ transitions in the framework of our first-order approximation. The importance of second-order contributions to all the observed transitions was demonstrated by a coupled channels calculation for the 0^+ , 2^+ , and 4^+ states.

II. EXPERIMENTAL TECHNIQUE AND RESULTS

The experiments were carried out at the 88-in. cyclotron of the Lawrence Berkeley Laboratory.

The energy of the ^{20}Ne beam was 50 MeV, corresponding to 22.2 MeV in the center of mass system. The average beam intensity was 100 nA on target; a collimator was used to fix the beam spot and reduce it to an area of about 2 mm^2 . Self-supporting targets of aluminum- and nickel-oxide with a thickness of 250 and $100 \mu\text{g}/\text{cm}^2$, respectively, were mounted in a scattering chamber equipped with a liquid nitrogen cooling finger close to the target as a trap for pump oil vapors, in order to reduce carbon buildup on the target during the experiment.

Two ΔE - E counter telescopes with $5 \mu\text{m}$ ORTEC ΔE transmission detectors and a solid angle of 2×10^{-4} sr were used along with a monitor detector. The telescope events were sent to a computer, stored in ΔE - $(E + \Delta E)$ arrays, and analyzed off line with a program for energy calibration, peak integration, peak unfolding, and background subtraction. Energy calibration of the spectra was obtained from the peak positions of the elastic ^{20}Ne scattering from ^{58}Ni , ^{27}Al , and ^{16}O . The overall energy resolution was about 500 keV, which was sufficient to separate the transitions to the ^{20}Ne ground state, 2^+ state at 1.63 MeV, and 4^+ state at 4.25 MeV. The corresponding peaks were identified by their kinematical shift with scattering angle from the peaks due to inelastic scattering and α transfer reactions on ^{27}Al and target impurities. For each scattering angle and telescope, both the spectra of outgoing ^{20}Ne and $^{16}\text{O}(\text{g.s.})$ products were obtained. Figure 1 shows these spectra for $\theta_{\text{lab}} = 36^\circ$. Since the $^{16}\text{O}(\text{g.s.})$ angular distributions at forward angles correspond to the angular distributions of the elastic and inelastic ^{20}Ne backward scattering it was sufficient to cover only the forward angles.

Angular distributions were measured in steps of 1° for angles between 10° and 48° in the lab sys-

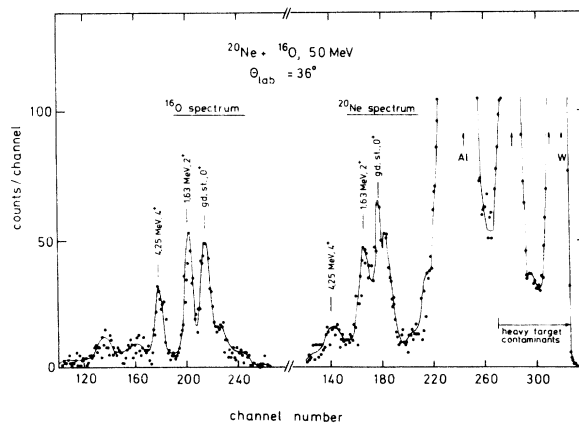


FIG. 1. Spectra of outgoing ^{20}Ne and ^{16}O at $\theta_{\text{lab}} = 36^\circ$.

tem, corresponding in the center of mass system to an angular region from 22.6° to 156° (for the ground-state transition) covered in steps of about 2.5° . Angular distributions for excited ^{20}Ne states above the 4^+ level, as well as for transitions to excited ^{16}O states, could not be obtained because the outgoing Ne products were stopped in the ΔE detectors. The NiO targets turned out to be very inhomogeneous and were only used for a few forward angles where the kinematic separation of the elastic peaks from ^{27}Al and ^{16}O was insufficient.

The relative normalization of the angular distributions was obtained from the beam charge integration in the Faraday cup and the monitor counter. Overlapping angles were taken to normalize the data from the NiO and Al_2O_3 targets to each other. The absolute cross section scale was obtained by normalizing the ^{20}Ne ground-state transition to an optical model calculation at forward angles where $\sigma \sim \sigma$ (Rutherford). The absolute cross sections were determined independently from the known solid angles by weighing an area of 1 cm^2 of the Al_2O_3 target. The results agreed to within 15%.

The resulting angular distributions for the ground state, 2^+ , and 4^+ states of ^{20}Ne are shown in Fig. 2. The error bars include errors due to statistics, background correction, and uncertainties in the unfolding of impurity peaks. For the 4^+ transition, the peaks could be identified with sufficient reliability only in the ^{16}O spectra, thus limiting the angular distribution to $\theta_{\text{c.m.}} \approx 70^\circ$.

A backward rise is observed in all three angular distributions, suggesting that a mechanism different from direct elastic or inelastic scattering takes over at angles beyond about 90° . The pronounced oscillations at intermediate angles, observed in the ground-state transition, appear damped in the inelastic reactions. The observed cross sections at about 160° are four times higher for the 2^+ and 4^+ transitions than for the ground state. This would be consistent with the assumption that the back angle cross section is due to a coherent α transfer contribution because ground-state $l=0$ transitions are usually kinematically suppressed in heavy-ion α transfer reactions on s - d shell nuclei at energies close to the Coulomb barrier.¹² In fact, the same ratio of 0^+ to 2^+ and 4^+ cross sections is observed¹³ in the reactions $^{16}\text{O}(^7\text{Li}, t)^{20}\text{Ne}$ and $^{16}\text{O}(^{16}\text{O}, ^{12}\text{C})^{20}\text{Ne}$.

Note that these relative reaction cross sections may be compared directly to ours because the α -spectroscopic factors should be approximately the same for all three states.^{1,4,5}

III. ANALYSIS OF THE DATA

For the quantitative analysis of our data, we will turn first to the ground-state transition and apply

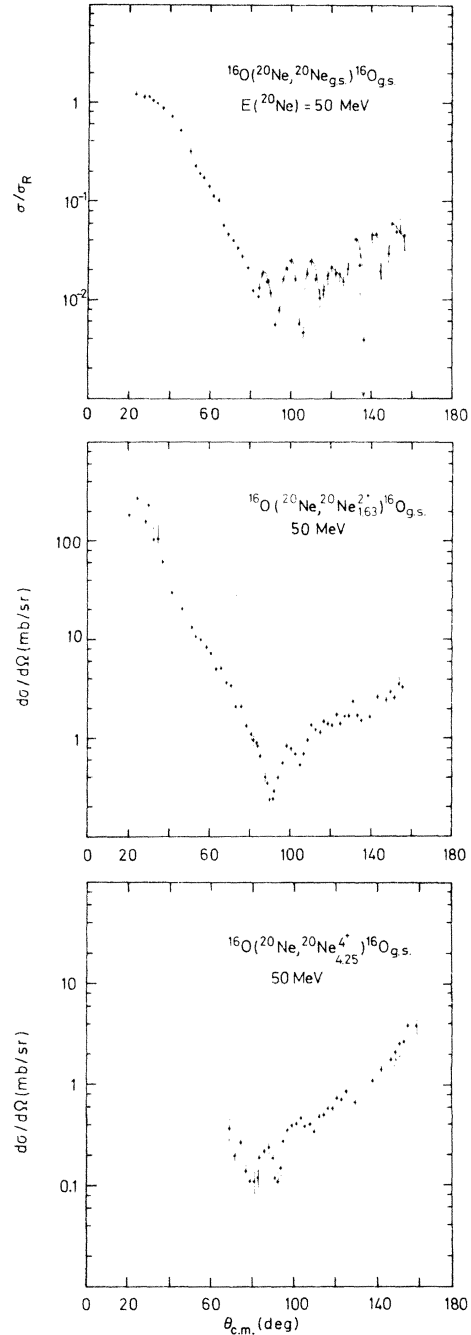


FIG. 2. Angular distributions for elastic and inelastic $^{20}\text{Ne} + ^{16}\text{O}$ scattering to the ground state, 2^+ (1.63 MeV), and 4^+ (4.25 MeV) states of ^{20}Ne . The smooth curve for the ground-state transition is drawn to guide the eye.

the optical model plus DWBA coherent superposition approximation^{8,9} (elastic transfer). In order to avoid *ad hoc* assumptions, the essential parameters were taken from systematic investigations of scattering and transfer reactions in the s - d

shell. Therefore, we used a standard set of optical model parameters that describe the average features of elastic scattering in the ^{16}O , ^{20}Ne region.¹⁴ Recoil effects in the DWBA transfer amplitude turned out to be very significant¹⁵; they were included using the quasiclassical approximation described by Braun-Munzinger and Harney.¹¹ Microscopic form factors and α -spectroscopic factors have been used to specify the α -cluster bound state wave function used in the DWBA amplitude.^{4,5} Nevertheless, no satisfactory fits were obtained, which is presumably due to the omission of second-order contributions to both the elastic and transfer amplitudes. Such second-order effects should be important because of the highly collective, deformed structure of the ^{20}Ne states involved. This was substantiated by a coupled channels calculation for the nonexchange part of the cross sections.

A. α -cluster relative motion form factors

In the DWBA treatment for four-nucleon transfer, the wave function φ_α for the bound nucleons is usually obtained as a cluster form factor from a Woods-Saxon (WS) potential by specifying the appropriate number of nodes and the separation energy of an asymptotically free α particle. The α -particle spectroscopic factor is then identified with the normalization integral of φ_α , i.e.,

$$S_\alpha^{\text{WS}} = \int |\varphi_\alpha(R)|^2 R^2 dR, \quad (3)$$

where R is the relative distance between cluster and core. S_α^{WS} is then determined by fitting the DWBA to the experimental cross section. For the ground state of ^{20}Ne , φ_α is given as the $5s$ state¹⁶ with separation energy $E_\alpha = -4.73$ MeV. No clear cut prescription exists for the choice of the radius and diffuseness parameters of the Woods-Saxon well. If they are taken to resemble closely the real part of the optical model that describes low energy α particle elastic scattering¹⁷ ($R_0 = r_0 A_{\text{core}}^{1/3}$ with $r_0 = 1.4$ fm, $a = 0.65$ fm), the resulting well depth is $V_0 = 114$ MeV.

From systematic DWBA studies of heavy-ion-induced four-nucleon transfer reactions such as (^{16}O , ^{12}C) at energies close to the Coulomb barrier it is known that the predicted cross sections are approximately proportional to the square of the bound state amplitude in the external region.¹² The insensitivity of peak cross sections to the interior parts of the wave functions results from the surface localization of direct transfer reactions.¹⁸ The essential features of the bound state form factor are, therefore, the slope which is unambiguously determined by the cluster separation energy, and the absolute magnitude in the ex-

ternal region. The latter depends on the overall normalization S_α and on the choice of the radius parameter R_0 of the Woods-Saxon well. Thus, the absolute value of S_α , extracted from a DWBA fit to the experimental cross section, depends strongly on R_0 and does not provide a well-defined result. However, relative spectroscopic factors for states belonging to the same intrinsic four nucleon configuration may be obtained by means of this procedure.³

In order to test the prediction of the first-order elastic transfer model for the $^{16}\text{O} + ^{20}\text{Ne}$ ground-state transition, together with the additional assumption that ^{20}Ne has a pure α -cluster configuration, the asymptotic part of the cluster form factor had to be unambiguously specified. A Woods-Saxon solution was therefore fitted to the external parts of various microscopic cluster model form factors by proper choice of S_α^{WS} and R_0 . The resulting WS solutions were then used in the recoil DWBA code to generate the exchange part of the elastic amplitude. This corresponds to specifying the α particle *reduced widths*, rather than the α -spectroscopic factor corresponding to the WS form factor, by the fit to the microscopic model relative-motion form factor. Because of the insensitivity of the transfer reaction cross section to the interior parts of the radial wave function, our approach does not imply that we consider the WS solution as an overall approximation to the microscopic form factor. As we shall show below, the amplitude of the latter is drastically reduced in the interior as an effect of the antisymmetrization. The WS solution used in the DWBA code serves only to reproduce the exterior part. The corresponding normalization S_α^{WS} is, therefore, more or less arbitrary; the α spectroscopic factor S_α is appropriately given by the normalization $S_\alpha^{\text{c.m.}}$ of the microscopic relative motion form factor [Eq. (2)].

Various microscopic α cluster model calculations for ^{20}Ne have been recently reviewed by Arima.¹ In general, the α -particle relative motion form factor is given by

$$\chi_L(R) = n_L \langle \Phi_\alpha \Phi_{\text{core}} Y_L | \alpha (\Phi_\alpha \Phi_{\text{core}} Y_L F_L(R)) \rangle, \quad (4)$$

where L is the cluster angular momentum, n_L a normalization factor, and the quantity in the right-hand side of the bracket is the antisymmetrized model wave function for ^{20}Ne . The relative motion part $F_L(R)$ is normalized to unity. The probability of finding an α particle in ^{20}Ne is then given by the normalization $S_\alpha^{\text{c.m.}}$ of $\chi_L(R)$ as given in Eq. (2). In most cases, it is smaller than unity due to the effect of antisymmetrization on $F_L(R)$. For example, describing the $K=0^+$ ground-state rotational band in the $(8, 0)$ representation of SU_3 ,

one finds¹ a maximum spectroscopic factor of $S_\alpha(8,0) = 0.23$. With j - j coupling wave functions and configuration mixing in the s - d shell, McGrory *et al.*¹⁹ obtained $S_\alpha^{\text{SM}} = 0.18$ for the ^{20}Ne ground state. Since the nucleons outside the ^{16}O core are limited to the s - d shell, in both cases, one may call a value of about 0.2 the shell model limit for S_α .

In order for S_α to approach unity, as is familiar for single nucleon spectroscopic factors, higher lying shell model orbits have to be admixed to the s - d shell, giving the α cluster a higher degree of localization than is implicit in the normal shell model wave function.¹ As $S_\alpha \rightarrow 1$, the cluster becomes more discernible in the nuclear density distribution and moves towards the surface. For the α - ^{16}O molecular rotator states,⁶ encountered in elastic α scattering from ^{16}O , clearly $S_\alpha \approx 1$. However, these are highly excited states; much less localization is possible in the ^{20}Ne ground state.

In our analysis of elastic transfer, we used wave functions obtained by Tomoda and Arima,⁵ and by Hiura, Nemoto, and Bando.⁴ In the model used by Tomoda and Arima, shell model wave functions with SU_3 representations $(\lambda, \mu) = (8, 0)$, $(10, 0)$, $(12, 0)$, and $(14, 0)$ are mixed into the relative motion function, assuming the ^{16}O core and the α cluster to be in their lowest internal states:

$$\Phi_L(^{20}\text{Ne}) = \sum_{\substack{\lambda \\ (2N+L=\lambda)}} a_L(\lambda) n_L \times \alpha(\Phi(^{16}\text{O})\Phi(\alpha)\Phi_{NL}(R_\alpha - R_{\text{core}})). \quad (5)$$

The coefficients $a_L(\lambda)$ are obtained with a Volkov 2 two-body potential, fitting the ^{20}Ne ground-state binding energy and the excitation spectrum of the $K = 0^+$ rotational band.

Hiura *et al.*⁴ start with a two-centered Brink-Bloch wave function

$$\Phi(^{20}\text{Ne}) = N(R_0, R_1)^{-1/2} \alpha(\Psi_{R_0}(^{16}\text{O})\Psi_{R_1}(\alpha)) \quad (6)$$

to which they apply angular momentum projection and the generator coordinate method with respect to $R = |R_0 - R_1|$, which represents the distance between the two clusters. Using the Volkov 2 two-body potential, they obtain satisfactory agreement with the ^{20}Ne excitation spectrum, and a ground-state α - ^{16}O binding energy of $E_B = -4.55$ MeV (the experimental value is $E_B = -4.73$ MeV). The cluster relative motion form factor of both models is obtained by the overlap integral (4); the spectroscopic factor $S_\alpha^{\text{c.m.}}$ is given by the normalization (2). The resulting $S_\alpha^{\text{c.m.}}$ for the ^{20}Ne ground state are 0.32 (Tomoda) and 0.45 (Hiura), respectively.

The corresponding cluster form factors are

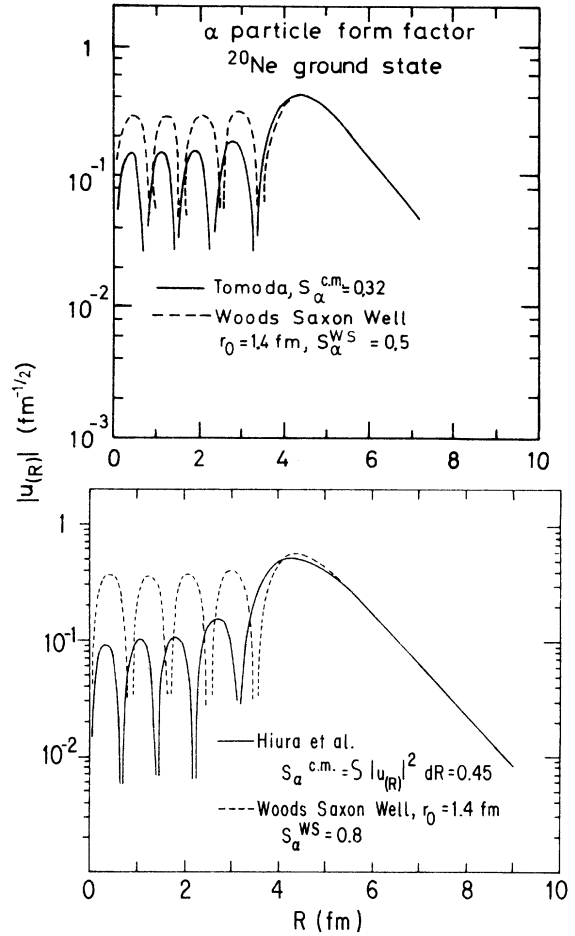


FIG. 3. α particle relative motion form factors for the ^{20}Ne ground state. Microscopic calculations of Tomoda and Arima (Ref. 5; upper part) and Hiura *et al.* (Ref. 4; lower part) are matched by Woods-Saxon solutions in the external region ($R > 5$ fm).

shown in Fig. 3, together with Woods-Saxon form factors obtained with $r_0 = 1.4$ fm that are normalized so as to fit the asymptotic parts ($R > 5$ fm). In the nuclear interior the microscopic form factors are drastically reduced due to the antisymmetrization, and the major part of the α particle probability amplitude is pushed into the surface region. The form factor of Hiura *et al.* with $S_\alpha^{\text{c.m.}} = 0.45$ exhibits the same surface amplitude as the Woods-Saxon form factor with $r_0 = 1.4$ and a normalization $S_\alpha^{\text{WS}} = 0.8$. The latter will be used in the DWBA analysis.

B. Elastic transfer and coupled channels calculations

The $^{16}\text{O} + ^{20}\text{Ne}$ ground-state transition was calculated as a coherent superposition of elastic scattering and cluster transfer using the code BRUNHILD of Braun-Munzinger, Harney, and Wenneis.²⁰ In

the reaction amplitude

$$T(\theta) = T(\theta)_{\text{OM}} + S_{\alpha} T_{\text{DWBA}}(\pi - \theta) \quad (7)$$

the relative phase is fixed by the symmetry of the system.⁸ The set of optical model parameters,¹⁴ used in both amplitudes, was $V_0 = 100$ MeV, $W = 35$ MeV, $r_v = r_w = 1.2$ fm, $a_v = 0.49$ fm, and $a_w = 0.32$ fm, representing a strongly absorbing potential. No l dependence of the absorption was taken into account because several direct exit channels are available to carry the grazing angular momentum $l_0 \approx 10$; among these the low lying collective states are particularly strongly excited in inelastic scattering (c.f. Fig. 2).

Effects of recoil and finite range should be highly important in the α - ^{16}O system because the transferred mass cannot be considered small relative to the core mass.¹⁵ This is different from the situation encountered in single nucleon elastic transfer reactions like $^{28}\text{Si} + ^{29}\text{Si}$ and precludes, in our case, the use of the LCNO model of von Oertzen and Nörenberg²¹ which does not incorporate recoil effects. The DWBA amplitude used in the code BRUNHILD treats recoil in the local momentum approximation, which is applicable to reactions with strong absorption in the entrance and exit channels where the reaction is localized to a radial domain outside the quasiclassical grazing radius.¹¹ In our calculations, the finite range and recoil effects led to a reduction of the extreme back angle cross section by almost an order of magnitude, and to a damping of the oscillatory structure at angles $\theta_{\text{c.m.}} \geq 120^\circ$.

The results of the optical model and elastic transfer calculations are compared with the ground-state transition data in Fig. 4. Both fits are identical for $\theta_{\text{c.m.}} \leq 80^\circ$; in this domain, the data are well reproduced. The OM cross section continues to fall off towards larger angles, in a manner typical for strongly absorbing potentials, whereas interference oscillations and a backward rise develop in the elastic transfer angular distribution for $\theta_{\text{c.m.}} > 80^\circ$. However, the experimental cross sections are largely underestimated at intermediate angles, where the phase of the oscillations is also not well reproduced.

A variation of the optical model parameters did not yield significant improvements insofar as a better agreement with the backward oscillatory pattern could only be achieved at the expense of fit quality at forward angles. Apparently, the DWBA amplitude falls off too rapidly from backward angles towards 90° , or the OM amplitude is inadequate for $\theta_{\text{c.m.}} > 80^\circ$. Attempts to improve the fit by scaling the DWBA amplitude with a larger bound state form factor normalization were unsuccessful. For example, an arbitrary normaliza-

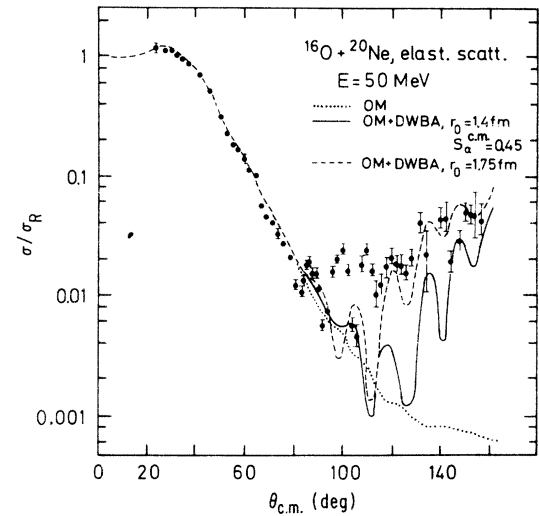


FIG. 4. Results of optical model (OM) and elastic transfer (OM+DWBA) calculations for the $^{20}\text{Ne} + ^{16}\text{O}$ ground-state transition.

tion to $S^{\text{WS}} = 2$ shifted the angular distribution upward by a uniform factor of about 4 for $\theta \geq 100^\circ$, improving the agreement at intermediate angles but far overestimating the cross sections at the very backward angles. A somewhat better overall fit was obtained by increasing the Woods-Saxon well radius from $r_0 = 1.4$ fm, as prescribed by the microscopic models, to $r_0 = 1.75$ fm, at the same time reducing the overall normalization to $S^{\text{WS}} = 0.5$. The corresponding fit is also shown in Fig. 4. However, this procedure implies an α -particle surface reduced width twice as high as given by the microscopic wave functions appropriate to the ^{20}Ne ground state. This corresponds to an α -cluster localization far beyond the limits indicated for low lying ^{20}Ne states by microscopic models.¹

It was therefore concluded that the first-order elastic scattering and exchange mechanism, underlying the OM plus DWBA approximation to elastic transfer, is not appropriate in the $^{16}\text{O} + ^{20}\text{Ne}$ case. An improved calculation would have to include virtual transitions to the excited collective states of ^{20}Ne both in the entrance and exit channels, as well as the transfer of the α cluster among excited states. No computer code was available to the authors that would take all these transitions into account, along with an appropriate treatment of recoil effects.

In order to demonstrate the higher order effects on the optical model amplitude alone, a coupled channels calculation was done for elastic and inelastic $^{16}\text{O} + ^{20}\text{Ne}$ scattering using the code of Ascuitto and Glendenning.²² No exchange contributions were taken into account. The usual collec-

tive macroscopic model was used²³ for the deformed nuclear field:

$$V(r-R(\theta)) = V(r-R) - \sum_{\lambda} \beta_{\lambda} Y_{\lambda} R_P \frac{\partial V}{\partial r} + \left(\sum_{\lambda} \beta_{\lambda} Y_{\lambda} \right)^2 \frac{1}{2} R_P^2 \frac{\partial^2 V}{\partial r^2} \mp \dots, \quad (8)$$

with

$$R(\theta) = R_T + R_P \left[1 + \sum_{\lambda} \beta_{\lambda} Y_{\lambda}^0(\theta) \right], \quad \lambda = 2, 4 \quad (9)$$

corresponding to a spherical ^{16}O with radius R_T , and a deformed ^{20}Ne projectile with radius R_P . All deformation constants are to be associated with the radius $R = 1.2(20)^{1/3}$. The deformation lengths $\beta^N R$ were taken from de Swiniarski *et al.*²⁴ The Coulomb deformation $\beta_2^C = 0.8$ was reduced slightly from the value 0.87 reported by Stelson

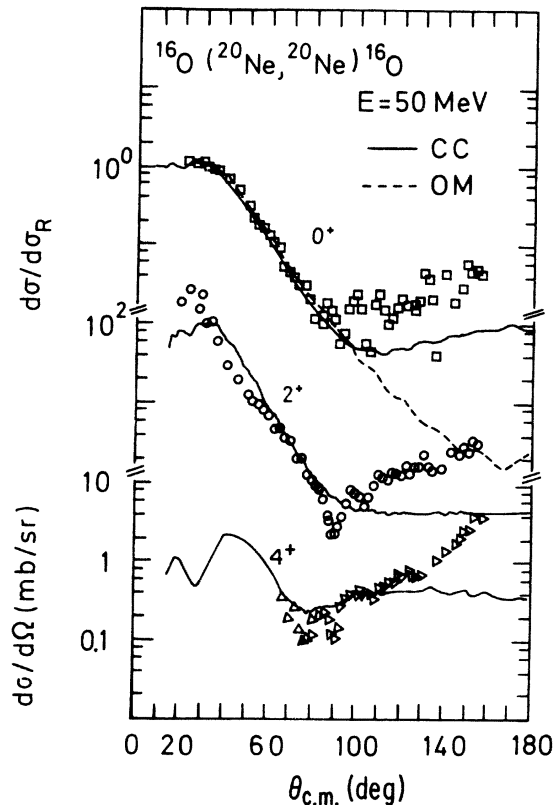


FIG. 5. Results of optical model (OM) and coupled channels (CC, no exchange) calculations for $^{20}\text{Ne} + ^{16}\text{O}$ scattering to the first three states in ^{20}Ne . Potential parameters are the same as in the elastic transfer calculation except $W = 15$ MeV. Deformation parameters are $\beta_2^N = 0.43$, $\beta_4^N = 0.26$, $\beta_2^C = 0.8$, and $\beta_4^C = 0.4$.

and Grodzins²⁵ because we include $\lambda = 4$ in the Coulomb field expansion, in addition to $\lambda = 2$.

The results of this calculation are shown in Fig. 5, which also gives the optical model fit (without channel coupling) for elastic scattering. The effect of channel coupling (CC) for the ground-state transition is clearly exhibited. At intermediate scattering angles where the elastic transfer calculation (Fig. 4) was systematically underestimating the observed cross section, the CC cross sections are much larger than the OM cross sections. The 2^+ transition cross section is underestimated at very forward angles. It should be noted, however, that we did not attempt any parameter optimization, and that the experimental error bars are large in this region (c.f. Fig. 2) due to normalization and background correction uncertainties.

IV. CONCLUSIONS

The shape and structure of the cross sections measured for the $^{20}\text{Ne} + ^{16}\text{O}$ scattering to the three lowest states of ^{20}Ne are in qualitative agreement with the assumption of an α -cluster exchange process dominating at backward angles. Calculations in the framework of a first-order optical model plus DWBA description of elastic transfer did not lead to quantitative agreement with our data, although microscopic form factors and recoil corrections were employed. The fits did not reproduce the interference structure at intermediate angles, indicating inadequacies in either the OM or the DWBA amplitudes, or both. The quality of the fit is better at forward and extreme backward angles where higher order corrections to the dominating amplitudes are less important. In such a limited sense, we may say that the α -particle spectroscopic factor $S_{\alpha}^{c.m.} = 0.45$ obtained for the ^{20}Ne ground state in the microscopic model of Hiura *et al.*⁴ is consistent with our data.

The coupled channels calculation for the ground state transition indicates that the OM amplitude is too small at backward angles. This may explain in part the low cross sections and wrong phases obtained in the intermediate angle elastic transfer calculations. One might therefore try to improve the model, replacing the OM amplitude in (7) by a coupled channel amplitude. This was not done for the following reasons:

- The higher order effects should be equally important for the transfer amplitude at intermediate angles (indirect transfer via excited states).
- The model would still be unsatisfactory as long as ^{20}Ne is treated macroscopically in the CC amplitude and microscopically in the DWBA transfer amplitude, resulting in difficulties in determining

the relative phases of the interfering amplitudes.

We may then hope that the present data and analysis will stimulate a more comprehensive theoretical investigation of the cluster exchange mechanism, leading to a reliable determination of the α -particle spectroscopic factor in the ^{20}Ne ground-state rotational band.

The authors would like to express their gratitude to the operating crew of the 88-in. cyclotron for their support, and to Dr. A. Arima, Dr. P. Braun-Munzinger, Dr. N. K. Glendenning, and Dr. F. Nemoto for providing us with their computer codes and microscopic wave functions, as well as for stimulating comments.

*Supported by the Bundesminister für Forschung und Technologie, German Federal Republic, and by the U. S. Research and Development Agency.

†Permanent address: Hahn Meitner Institut für Kernforschung, Berlin, West Germany.

‡Now at Vanderbilt University, Nashville, Tennessee.

§Permanent address: Gesellschaft für Schwerionenforschung, Darmstadt, West Germany.

¶Present address: Fachbereich Physik, Technische Hochschule Darmstadt, West Germany.

¹A. Arima, in *Proceedings of the International Conference on Nuclear Physics, Munich, 1973*, edited by J. de Boer and H. J. Mang (North-Holland, Amsterdam/American Elsevier, New York, 1973), Vol. 2, p. 183.

²M. Ichimura, A. Arima, E. C. Halbert, and T. Terasawa, *Nucl. Phys.* **A204**, 225 (1973).

³K. I. Kubo, F. Nemoto, and H. Bando, *Nucl. Phys.* **A224**, 573 (1974).

⁴J. Hiura, F. Nemoto, and H. Bando, *Progr. Theor. Phys. Suppl.* **52**, 173 (1972); F. Nemoto (private communication).

⁵T. Tomoda and A. Arima, in *Proceedings of the INS-IPCR Symposium on Cluster Structure, Toyko, 1975*, edited by H. Kamitsubo *et al.* (unpublished), p. 90; and private communication.

⁶W. Sünkel and K. Wildermuth, *Phys. Lett.* **41B**, 439 (1972).

⁷W. von Oertzen and H. G. Bohlen, *Phys. Rep.* **19C**, 1 (1975).

⁸P. Braun-Munzinger *et al.*, *Z. Phys.* **A276**, 107 (1976); W. F. W. Schneider *et al.* *Phys. Lett.* **46B**, 195 (1973).

⁹G. Baur and C. K. Gelbke, *Nucl. Phys.* **A204**, 138 (1973); W. Bohne *et al.*, *Nucl. Phys.* **A222**, 117 (1974).

¹⁰K. D. Hildenbrand *et al.*, *Nucl. Phys.* **A234**, 167 (1974).

¹¹P. Braun-Munzinger and H. L. Harney, *Nucl. Phys.*

A223, 381 (1974).

¹²W. von Oertzen, in *Nuclear Spectroscopy*, edited by J. Cerny (Academic, New York, 1974), Part B, p. 279.

¹³R. Middleton, B. Rosner, D. J. Pullen, and L. Polsky, *Phys. Rev. Lett.* **20**, 118 (1968); H. T. Fortune, R. R. Betts, J. D. Garrett, and R. Middleton, *Phys. Lett.* **44B**, 65 (1973); J. P. Draayer *et al.*, *Phys. Lett.* **53B**, 250 (1974); H. H. Gutbrod, Ph.D. thesis, Heidelberg, 1970 (unpublished).

¹⁴R. H. Siemssen, H. T. Fortune, A. Richter, and J. W. Tippie, *Phys. Rev. C* **5**, 1839 (1972).

¹⁵J. S. Blair *et al.*, *Phys. Rev. C* **10**, 1856 (1974).

¹⁶The $5s$, $L=0$ relative motion form factor has four radial nodes (excluding that for $R \rightarrow \infty$, and at the origin); according to the SU_3 classification $2N+L=8$.

¹⁷G. Gaul *et al.*, *Nucl. Phys.* **A137**, 177 (1969).

¹⁸R. Stock *et al.*, *Nucl. Phys.* **A104**, 136 (1967).

¹⁹J. B. McGrory, in *Proceedings of the International Conference on Nuclear Physics, Munich, 1973*, edited by J. de Boer and H. J. Mang (North-Holland, Amsterdam/American Elsevier, New York, 1973), Vol. 2, p. 145, and references therein.

²⁰P. Braun-Munzinger, H. L. Harney, and S. Wenneis, *Nucl. Phys.* **A235**, 190 (1974); S. Wenneis, P. Braun-Munzinger, and H. L. Harney, Max Planck Institute Report No. MPIH-1974-V19 (unpublished).

²¹W. von Oertzen and W. Nörenberg, *Nucl. Phys.* **A207**, 113 (1973).

²²R. J. Ascutto and N. K. Glendenning, *Phys. Rev.* **181**, 1396 (1969).

²³N. K. Glendenning and G. Wolschin, LBL Berkeley Report No. 4341 (unpublished).

²⁴R. de Swiniarski *et al.*, *Phys. Lett.* **43B**, 27 (1973).

²⁵R. H. Stelson and L. Grodzins, *Nucl. Data* **A1**, 21 (1965).